

Harteneck et al.<sup>[22]</sup> The antibodies used are directed against the C-terminal peptide of the  $\alpha_2$  subunit (KKVSYNIGTTMFLRETSL).

Received: December 23, 1998 [Z 12821 IE]  
German version: *Angew. Chem.* **1999**, *111*, 2180–2184

**Keywords:** molecular recognition • peptides • peptide–peptide interactions

- [1] P. Bork, J. Schultz, C. P. Ponting, *Trends Biochem. Sci.* **1997**, *22*, 296–298.
- [2] P. Bork, E. V. Koonin, *Curr. Opin. Struct. Biol.* **1996**, *6*, 366–376.
- [3] a) J. K. Scott, G. P. Smith, *Science* **1990**, *249*, 386–390; b) S. Fields, O. Song, *Nature* **1989**, *340*, 245–246.
- [4] a) K. O. Cho, C. A. Hunt, M. B. Kennedy, *Neuron* **1992**, *9*, 929–942; b) C. P. Ponting, C. Phillips, *Trends Biochem. Sci.* **1995**, *20*, 102–103; c) C. P. Ponting, C. Phillips, K. E. Davies, D. J. Blake, *BioEssays* **1997**, *19*, 469–479.
- [5] J. E. Brenman, S. S. Chao, S. H. Gee, A. W. McGee, S. E. Craven, D. R. Santillano, Z. Wu, F. Huang, H. Xia, M. F. Peters, S. C. Froehner, D. S. Brendt, *Cell* **1996**, *84*, 757–767.
- [6] J. Saras, C. Heldin, *Trends Biochem. Sci.* **1996**, *21*, 455–458.
- [7] a) R. Frank, *Tetrahedron* **1992**, *48*, 9217–9232; b) R. Frank, H. Overwin, *Methods Mol. Biol.* **1996**, *66*, 149–169; c) A. Kramer, J. Schneider-Mergener, *Methods Mol. Biol.* **1998**, *87*, 25–39.
- [8] a) R. S. Kania, R. N. Zuckermann, C. K. Marlowe, *J. Am. Chem. Soc.* **1994**, *116*, 8835–8836; b) M. Lebl, V. Krchnak, N. F. Sepetov, V. Nikolaev, A. Stieradova, P. Safar, B. Seligmann, P. Stop, P. Thorpe, S. Felder, D. F. Lake, K. S. Lam, S. E. Salmon in *Innovation and Perspectives in Solid Phase Synthesis* (Ed.: R. Epton), Mayflower Worldwide, Oxford, **1994**, p. 233.
- [9] M. E. Adams, T. M. Dwyer, L. L. Dowler, R. A. White, S. C. Froehner, *J. Biol. Chem.* **1995**, *270*, 25859–25865.
- [10] J. Schultz, U. Hoffmüller, G. Krause, J. Ashurst, M. Macias, P. Schmieder, J. Schneider-Mergener, H. Oschkinat, *Nat. Struct. Biol.* **1998**, *5*, 19–24.
- [11] S. H. Gee, R. Madhavan, S. R. Levinson, J. H. Caldwell, R. Sealock, S. C. Froehner, *J. Neurosci.* **1998**, *18*, 128–137.
- [12] a) L. Fu, G. Wallukat, A. Hjalmarson, J. Hoebeke, *Clin. Exp. Immunol.* **1994**, *97*, 146–151; b) A. H. Ahn, C. A. Freener, E. Gussoni, M. Yoshida, E. Ozawa, L. M. Kunkel, *J. Biol. Chem.* **1996**, *271*, 2724–2730.
- [13] D. Koesling, J. Herz, H. Gausepohl, F. Niroomand, K. D. Hinsch, A. Mulsch, E. Böhme, G. Schultz, R. Frank, *FEBS Lett.* **1988**, *239*, 29–34.
- [14] D. S. Chao, F. Silvagno, H. Xia, T. L. Corwell, T. M., Lincoln, D. S. Bredt, *Neuroscience* **1997**, *76*, 665–672.
- [15] T. C. Liang, W. Luo, J. T. Hsieh, S. H. Lin, *Arch. Biochem. Biophys.* **1996**, *329*, 208–14.
- [16] M. Davies, M. Bradley, *Angew. Chem.* **1997**, *109*, 1135–1138; *Angew. Chem. Int. Ed. Engl.* **1997**, *36*, 1097–1099.
- [17] R. Volkmer-Engert, B. Hoffmann, J. Schneider-Mergener, *Tetrahedron Lett.* **1997**, *38*, 1029–1032.
- [18] M. B. Wilson, P. K. Nakane in *Immunofluorescence Related Staining Techniques* (Eds.: W. Knapp, K. Hlubar, G. Wick), Elsevier, Amsterdam, **1978**, pp. 215–224.
- [19] B. Friguet, A. F. Chaffotte, L. Djavadi-Ohanian, M. E. Goldberg, *J. Immunol. Methods* **1985**, *77*, 305–319.
- [20] M. Russwurm, S. Behrends, C. Harteneck, D. Koesling, *Biochem. J.* **1998**, *335*, 125–130.
- [21] M. M. Bradford, *Anal. Biochem.* **1976**, *72*, 248–254.
- [22] C. Harteneck, B. Wedel, D. Koesling, J. Malkewitz, E. Böhme, G. Schultz, *FEBS Lett.* **1991**, *292*, 217–222.
- [23] M. Michalak, M. Opas, *Curr. Opin. Neurol.* **1997**, *10*, 436–42.
- [24] A. Castello, V. Brocheriou, P. Chafey, A. Kahn, H. Gilgenkrantz, *FEBS Lett.* **1996**, *383*, 124–128.

## N<sub>5</sub><sup>+</sup>: A Novel Homoleptic Polynitrogen Ion as a High Energy Density Material\*\*

Karl O. Christe,\* William W. Wilson,  
Jeffrey A. Sheehy, and Jerry A. Boatz

*Dedicated to Professor George Olah*

Polynitrogen compounds are of significant interest as high energy density materials (HEDM) for propulsion or explosive applications.<sup>[1–3]</sup> In spite of numerous theoretical studies predicting that certain all-nitrogen compounds might be stable, only a few unsuccessful experimental studies aimed at their actual synthesis have been undertaken.<sup>[4]</sup> Presently, only two homoleptic polynitrogen species are known that can be prepared on a macroscopic scale: dinitrogen, N<sub>2</sub>, which was independently isolated in pure form from air in 1772 by Rutherford, Scheele, and Cavendish, and the azide anion, N<sub>3</sub><sup>−</sup>, discovered in 1890 by Curtius.<sup>[5]</sup> Other species such as N<sub>3</sub><sup>•</sup>, N<sub>3</sub><sup>+</sup>, and N<sub>4</sub><sup>+</sup> have been observed only as free gaseous or matrix-isolated ions or radicals.<sup>[6–8]</sup> In view of the extensive theoretical studies indicating that molecules such as N<sub>4</sub>, N<sub>8</sub>, N(N<sub>3</sub>)<sub>2</sub><sup>−</sup>, N(N<sub>3</sub>)<sub>3</sub>, and N(N<sub>3</sub>)<sub>4</sub><sup>+</sup> are vibrationally stable,<sup>[4]</sup> the lack of a single successful synthesis of a new species on a macroscopic scale is surprising and may be a testament to the great experimental difficulties resulting from their high endothermicities, which give rise to instability and unpredictable explosiveness.

The high energy content of polynitrogen candidates stems from the N–N single and double bonds they possess. The average bond energies of 160 and 418 kJ mol<sup>−1</sup>, respectively, are much less than one-third or two-thirds the N<sub>2</sub> triple bond energy of 954 kJ mol<sup>−1</sup>.<sup>[9]</sup> Therefore, any transformation of a polynitrogen compound to N<sub>2</sub> molecules is accompanied by a very large energy release, and any new metastable polynitrogen compound will be isolable and manageable only if it possesses a sufficiently large energy barrier to decomposition.

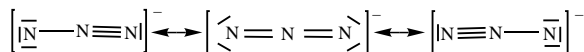
In view of the dearth of potential synthetic pathways for the construction of homoleptic polynitrogen rings or polycycles, and because many chain- or branch-type polynitrogen compounds are calculated to be lower in energy than their cyclic or polycyclic isomers,<sup>[3]</sup> our efforts are focused on the synthesis of catenated polynitrogen species, which may be more readily accessible. The weakest link in a chain always

[\*] Dr. K. O. Christe, Dr. W. W. Wilson, Dr. J. A. Sheehy, Dr. J. A. Boatz  
Propulsion Sciences and Advanced Concepts Division  
Air Force Research Laboratory (AFRL/PRS)  
Edwards Air Force Base, CA 93524 (USA)  
Fax: (+1) 661-275-5471  
E-mail: karl.christe@ple.af.mil  
and  
Loker Hydrocarbon Research Institute  
University of Southern California  
Los Angeles, CA 90089 (USA)

[\*\*] This work was funded predominantly by the Defense Advanced Research Projects Agency, with additional support from the Air Force Office of Scientific Research and the National Science Foundation. We thank A. Kershaw for recording the NMR spectra, Dr. M. Fajardo for the mass spectra, Prof. J. Stanton for calculating the nitrogen NMR shifts, and Dr. P. Carrick, Dr. S. Rodgers, Dr. M. Berman, and Dr. A. Morrish for continuing encouragement and support.

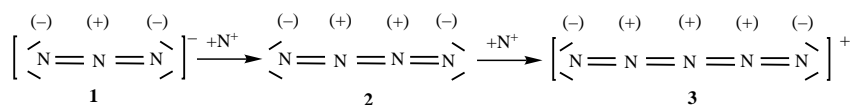
determines the overall strength, so it is imperative to search for target compounds devoid of any isolated N–N single bonds that cannot gain partial multiple bond character through resonance with neighboring bonds.

The building principle and unique resonance stabilization of the well-known and exceptionally stable azide anion (**1**, Scheme 1), in which each N–N bond has full double bond



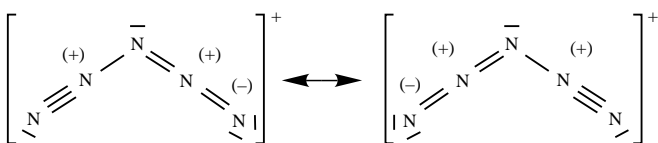
Scheme 1. Resonance structures of  $\text{N}_3^-$  (**1**).

character, might be further extended by the addition of nitrogen atoms containing only four valence electrons, that is,  $\text{N}^+$  ions. This leads first to neutral  $\text{N}_4$  (**2**) and then to the  $\text{N}_5^+$  cation (**3**, Scheme 2).



Scheme 2. Addition of  $\text{N}^+$  to  $\text{N}_3^-$  (**1**) to form  $\text{N}_4$  (**2**) and  $\text{N}_5^+$  (**3**) as well as the electronic charge distributions in **1**–**3**.

Although **2** and **3** contain, like azide, only cumulated linear N=N bonds, the electronic charge distributions shown in Scheme 1 are only favorable for  $\text{N}_3^-$ , whereas the neighboring positive charges render structures **2** and **3** energetically unfavorable. However, the problem of neighboring equal-sign charges can be remedied for  $\text{N}_5^+$  with the resonance structures shown in Scheme 3, which result in a bent structure of  $C_{2v}$  symmetry with a bond order of 1.5 for the central N–N bonds. For linear  $\text{N}_4$ , analogous structures cannot be written, and therefore  $\text{N}_5^+$  was chosen as the prime target of our synthesis program.



Scheme 3. Resonance structures of  $\text{N}_5^+$  (**3**).

Only one previous report on  $\text{N}_5^+$  was found in the literature, a theoretical study of a series of ABCBA-type compounds by Pyykkö and Runeberg.<sup>[10]</sup> Based on MP2/6-31G\* calculations, they predicted a planar  $C_{2v}$ -symmetric structure with a B–C–B angle of  $110.7^\circ$ . The possible synthesis of  $\text{N}_5^+$  was considered in 1992 by G. Rasul in his Ph.D. proposal at the University of Southern California, but it was not pursued.<sup>[11]</sup> Theoretical calculations were used to predict whether the candidate is vibrationally stable, and IR, Raman, and NMR spectra were calculated to aid in the identification and characterization. For  $\text{N}_5^+$ , these calculations predict the stable  $C_{2v}$  structure depicted in Figure 1. We report now the synthesis and characterization of  $\text{N}_5^+\text{AsF}_6^-$ , which constitutes only the third known compound containing a homoleptic polynitrogen moiety that is preparable on a macroscopic scale.

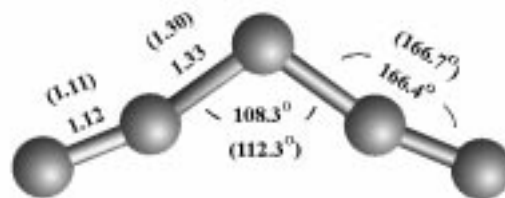
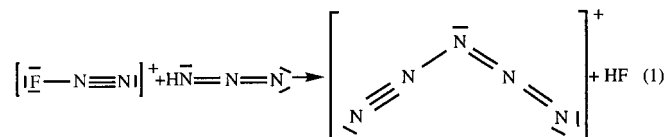


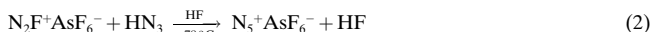
Figure 1. Optimized structures of  $\text{N}_5^+$  calculated at the B3LYP (values given in parentheses) and CCSD(T)/6-311 + G(2d) levels of theory.

In designing a synthesis, it is useful to find energetic starting materials that already possess the energy-enhancing weakened bonds, the required formal charges, and suitable ligands that allow for an exothermic and facile coupling reaction. If the target molecule is a cation such as  $\text{N}_5^+$ , the presence of a formal positive charge in one of the starting materials is very important in view of the high first ionization potential of  $\text{N}_2$  ( $1503 \text{ kJ mol}^{-1}$ ). Equation (1) shows that the  $\text{N}_2\text{F}^+$  cation and  $\text{HN}_3$  are ideal starting materials for the synthesis of  $\text{N}_5^+$  because they already possess the desired types of bonds,  $\text{N}_2\text{F}^+$  provides the formal positive charge, and, in view of the weak N–F and strong H–F bond, the HF elimination reaction is expected to be exothermic.



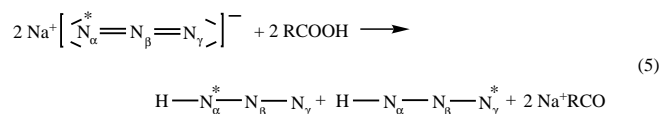
A final important point is the need for a reaction medium that offers good solubility at low temperatures, can act as a heat sink for the exothermic reaction, and can stabilize a product that is potentially very shock sensitive. For  $\text{N}_5^+$ , anhydrous HF was chosen because of its high dipole moment, low melting point ( $-80^\circ\text{C}$ ), and high volatility.

Application of these principles led to a surprisingly straightforward synthesis of  $\text{N}_5^+$  according to Equation (2). A

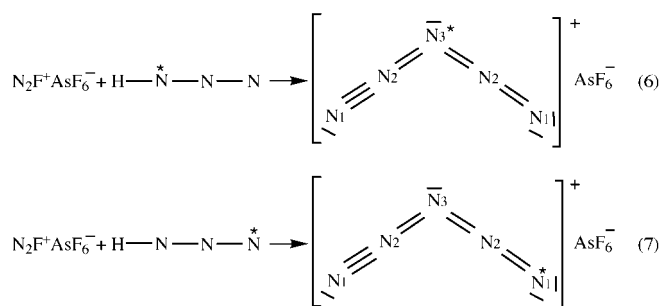


small excess of  $\text{HN}_3$  was used to ensure complete conversion of the  $\text{N}_2\text{F}^+\text{AsF}_6^-$ . The only detectable by-product was less than 20 mol% of protonated  $\text{HN}_3$ ,<sup>[12]</sup> formed according to Equation (3). The  $\text{AsF}_5$  required for the protonation of  $\text{HN}_3$  to proceed could have formed by decomposition of some  $\text{N}_5^+\text{AsF}_6^-$ , or less likely by hydrolysis of  $\text{N}_5^+\text{AsF}_6^-$  with traces of water in the system [Eq. (4)].

For the synthesis of  $^{15}\text{N}$ -labeled  $\text{N}_5^+$ ,  $^{15}\text{N}$ -labeled  $\text{HN}_3$  was prepared from stearic acid and  $^{15}\text{N}$ -labeled  $\text{Na}^+\text{N}_3^-$  [Eq. (5)].



The reaction of labeled  $\text{HN}_3$  with  $\text{N}_2\text{F}^+\text{AsF}_6^-$  produced a roughly equimolar mixture of  $\text{N}_5^+$  with  $^{15}\text{N}$  in either the 1- or 3-position [Eqs. (6), (7)].



The  $\text{N}_5^+\text{AsF}_6^-$  salt is a white solid that is sparingly soluble in anhydrous HF. It is marginally stable at  $22^\circ\text{C}$  and can be stored for weeks at  $-78^\circ\text{C}$  without noticeable decomposition. It can be handled both in HF solution or as a solid and, in our experience, has not exploded during careful normal handling or when squashed with a stainless steel spatula at  $-196^\circ\text{C}$ . It has survived numerous exposures to a focused 488-nm Ar-ion laser beam (1.5 watt) at  $-130^\circ\text{C}$ , although a 5-mg sample did explode on one occasion with sufficient force to destroy our low-temperature Raman device. It is a powerful oxidizer, capable of igniting organic substances such as foam rubber even at low temperatures. The reaction of  $\text{N}_5^+\text{AsF}_6^-$  with water is violently explosive and should be avoided. This is not surprising in view of the facts that  $\text{O}_2^+$  is a powerful oxidizer and the first ionization potential of  $\text{N}_2$  ( $1503 \text{ kJ mol}^{-1}$ ) is significantly higher than that of  $\text{O}_2$  ( $1206 \text{ kJ mol}^{-1}$ ); the electron affinity of  $\text{N}_5^+$  is the subject of a further computational study. The high energy density of  $\text{N}_5^+$  was also confirmed by a calculation using the G2 method<sup>[13]</sup> that gave formation enthalpies of  $\Delta H_f^0 = 1478$  and  $\Delta H_f^0 = 1469 \text{ kJ mol}^{-1}$  for free gaseous  $\text{N}_5^+$ .

Solid  $^{15}\text{N}$ -labeled  $\text{N}_5^+\text{AsF}_6^-$  in a quartz tube (3 mm outer diameter) was warmed in a stepwise manner from  $-78$  to  $+22^\circ\text{C}$  under a vacuum of  $10^{-7}$  Torr while monitoring the volatile products with a mass spectrometer; the principal decomposition product detected was  $\text{N}_2$ . After pumping at  $22^\circ\text{C}$  for 20 min, however, most of the solid remained and was identified by low-temperature Raman spectroscopy as  $\text{N}_5^+\text{AsF}_6^-$ , thus demonstrating that the compound has reasonable stability at room temperature. In samples prepared from an excess of  $\text{HN}_3$  and containing some  $\text{H}_2\text{N}_3^+\text{AsF}_6^-$ <sup>[12]</sup> as a by-product,  $\text{HN}_3$  and its fragments, HF, and  $\text{AsF}_5$  were also observed in the mass spectra.

The  $^{14}\text{N}$  and  $^{15}\text{N}$  NMR spectra of  $\text{N}_5^+$  labeled in either the 1- or 3-position and the  $^{14}\text{N}$  NMR spectrum of unlabeled  $\text{N}_5^+$  were recorded at  $-63^\circ\text{C}$  in anhydrous HF solution that was acidified with about 2 mol % of  $\text{AsF}_5$  to slow down a potential exchange between the cation and the solvent.<sup>[14]</sup> The spectra of the  $^{15}\text{N}$ -labeled mixture are shown in Figure 2, and the observed and calculated chemical shifts are compared in Table 1.

The signals due to N1 and N3 were observable in the  $^{15}\text{N}$  spectra at  $\delta = -237.3$  and  $-100.4$ , respectively, in excellent

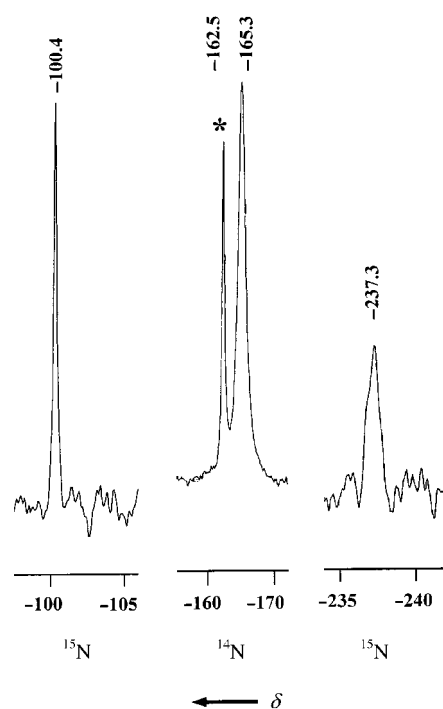


Figure 2. Sections of  $^{14}\text{N}$  and  $^{15}\text{N}$  NMR spectra for an equimolar mixture of singly  $^{15}\text{N}$ -labeled  $[\text{N}_5^+]$  and  $[\text{N}_5^+]\text{AsF}_6^-$  recorded at  $-63^\circ\text{C}$  in anhydrous HF solution that was acidified with 2 mol %  $\text{AsF}_5$ . The resonance marked by an asterisk is due to  $\text{H}_2\text{N}_3^+$  (see text for details).

Table 1. Observed and calculated  $^{15}\text{N}$  and  $^{14}\text{N}$  NMR data for  $\text{N}_5^+$ .

	$\delta$ <sup>[a]</sup>			
	observed <sup>[b]</sup> $^{15}\text{N}$	$^{14}\text{N}$	calculated <sup>[c]</sup> N1	calculated <sup>[c]</sup> N2 N3
$[\text{N}_5^+]$				
$[\text{N}_5^+]$	-237.3			
		-165.3 <sup>[d]</sup>	-235	-166 -95
$[\text{N}_5^+]$				
$[\text{N}_5^+]$	-100.4			

[a] Chemical shifts are given relative to that of neat  $\text{CH}_3\text{NO}_2$  as external standard. [b] The spectra were recorded  $^1\text{H}$ -coupled at  $-63^\circ\text{C}$  in anhydrous HF solution which was acidified with  $\text{AsF}_5$ . [c] Calculated at the CCSD(T)/QZP level of theory. An empirical correction of  $-20$  ppm was applied to all calculated values, based on a comparison between the calculated and observed shifts of a number of closely related molecules and ions. [d] The other two resonances are badly broadened owing to exchange and were not detected in the  $^{14}\text{N}$  spectrum.

agreement with the calculated values of  $\delta = -235$  and  $-95$ . The signal-to-noise ratio of the  $^{15}\text{N}$  spectrum was low due to the poor solubility of  $\text{N}_5^+\text{AsF}_6^-$  in HF at  $-63^\circ\text{C}$ , and a long delay time (60 s) was needed because of the slow relaxation rates. The area ratio of the two signals was about 1:1, indicating that the synthesis of  $\text{HN}_3$  from end-labeled  $\text{N}_3^-$  and stearic acid had resulted in about equimolar quantities of  $\text{N}_\alpha^-$  and  $\text{N}_\gamma^-$ -labeled  $\text{HN}_3$ . In addition to the two  $\text{N}_5^+$  signals, two weaker signals at  $\delta = -312.0$  (t,  $^1J(^1\text{H}, ^{15}\text{N}) = 100.7 \text{ Hz}$ ) and  $-111.4$  (s) were observed in the  $^1\text{H}$ -coupled  $^{15}\text{N}$  NMR spectrum that are attributable to  $\text{N}_\alpha$  and  $\text{N}_\gamma$ , respectively, of  $[\text{H}_2\text{N}_\alpha\text{N}_\beta\text{N}_\gamma]^+$ .<sup>[12]</sup> This was verified by recording the spectrum of a known sample of  $\text{H}_2\text{N}_3^+\text{AsF}_6^-$  in HF solution.

In the  $^{14}\text{N}$  spectrum of labeled and unlabeled  $\text{N}_5^+\text{AsF}_6^-$  a single resonance at  $\delta = -165.3$  was observed and assigned to

N2 of  $N_5^+$  based on the calculated value of  $\delta = -166$ . The signals due to N1 and N3 could not be observed in the  $^{14}\text{N}$  spectra under these conditions due to excessive quadrupole broadening. The  $N_\beta$  signal of  $[\text{H}_2\text{N}_\alpha\text{N}_\beta\text{N}_\gamma]^+$  was also observable in the  $^{14}\text{N}$  spectra of the labeled and unlabeled cations as a sharp resonance at  $\delta = -162.5$ , while signals for  $N_\alpha$  and  $N_\gamma$  were strongly quadrupole broadened. It is fortunate that N2 of  $N_5^+$  gives rise to a sharp  $^{14}\text{N}$  signal and that the single  $^{15}\text{N}$  substitution provided us with an equal mixture of  $^{15}\text{N}$  labels on N1 and N3, thus allowing the unambiguous observation of all three signals of  $N_5^+$ . Their excellent agreement with the calculated values provides positive proof for the presence of a  $C_{2v}$ -symmetric  $N_5^+$  cation.

Additional unambiguous proof for the presence of  $C_{2v}$ - $N_5^+$  was provided by the vibrational spectra of  $N_5^+\text{AsF}_6^-$  and the  $^{14}\text{N}$ – $^{15}\text{N}$  isotopic shifts observed for the mixture of  $^{15}\text{N}1$ - and  $^{15}\text{N}3$ -labeled  $N_5^+\text{AsF}_6^-$ . The low-temperature Raman spectra of unlabeled and a mixture of labeled  $N_5^+\text{AsF}_6^-$  are shown in Figures 3 and 4, respectively, and the observed frequencies are summarized in Tables 2 and 3. The vibrational assignments for octahedral  $\text{AsF}_6^-$  in Table 2 are well established<sup>[15]</sup> and do not

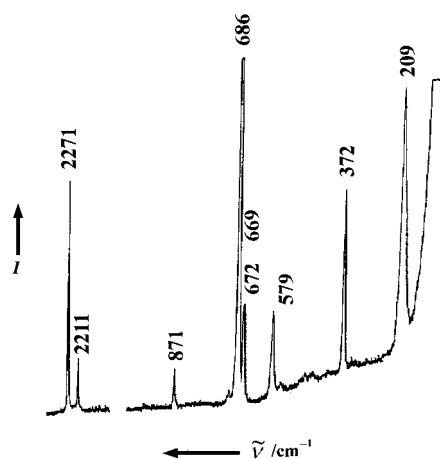


Figure 3. Low-temperature Raman spectrum of unlabeled solid  $N_5^+\text{AsF}_6^-$ .

require any further discussion; those for  $N_5^+$  are based on our calculations. As can be seen, the four N–N stretching modes were observed with the predicted frequencies and intensities.

The spectra of  $^{15}\text{N}1$ - and  $^{15}\text{N}3$ -labeled  $N_5^+$  allowed accurate measurements of the isotopic shifts for modes  $\nu_2(A_1)$ ,  $\nu_7(B_2)$ , and  $\nu_1(A_1)$ . Again, the agreement between experiment and theory is very good and confirms the validity of the predicted structure given in Figure 1. Since the observed frequencies of  $N_5^+$  are intermediate between those predicted at the CCSD(T) and the B3LYP levels of calculation, the actual geometry of  $N_5^+$  is probably also intermediate between the CCSD(T) and B3LYP values of Figure 1. Therefore, the following geometry is interpolated for  $[\text{N}1\text{--N}2\text{--N}3\text{--N}2\text{--N}1]^+$ :  $r(\text{N}1\text{--N}2) = 1.11 \text{ \AA}$ ,  $r(\text{N}2\text{--N}3) = 1.315 \text{ \AA}$ ,  $\angle(\text{N}1\text{--N}2\text{--N}3) = 166.6^\circ$ , and  $\angle(\text{N}2\text{--N}3\text{--N}2) = 110.3^\circ$ .

The results from a normal coordinate analysis of  $N_5^+$  are summarized in Table 4. They show that the  $A_2$ ,  $B_1$ , and  $B_2$  vibrations and  $\nu_1(A_1)$  are all highly characteristic, but that  $\nu_2(A_1)$  is a mixture of stretches and bends.

The internal force constants of greatest interest are the stretching force constants  $f_r$  and  $f_R$  of the terminal and the central N–N bonds, respectively. Interpolation of the data in Table 4 and adjustments for the observed frequencies give values of 20.08 and 6.59  $\text{mdyn \AA}^{-1}$  for the terminal and the central N–N stretching force constants, respectively. The

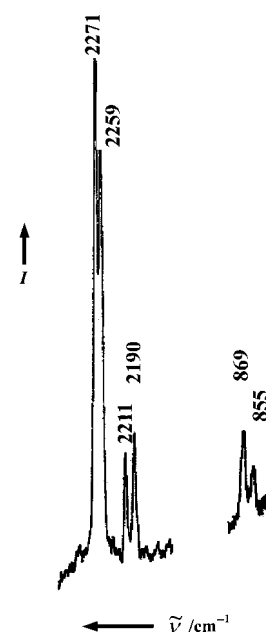


Figure 4. Low-temperature Raman spectrum of an equimolar mixture of solid  $[\text{N}^{15}\text{N}^{14}\text{N}^{14}\text{N}^{14}\text{N}^{14}\text{N}^{14}]^+\text{AsF}_6^-$  and  $[\text{N}^{14}\text{N}^{14}\text{N}^{15}\text{N}^{14}\text{N}^{14}\text{N}^{14}]^+\text{AsF}_6^-$ .

Table 2. Low-temperature Raman and IR bands of solid  $^{14}\text{N}_5^+\text{AsF}_6^-$  and their assignments based on the calculated harmonic frequencies of free gaseous  $N_5^+$ .

Obsd frequencies [ $\text{cm}^{-1}$ ] <sup>[a]</sup>		Assignment (point group)		Calcd frequencies [ $\text{cm}^{-1}$ ] <sup>[b]</sup>	
Raman <sup>[c]</sup>	IR <sup>[d]</sup>	$^{14}\text{N}_5^+(C_{2v})$	$\text{AsF}_6^-(O_h)$	B3LYP	CCSD(T)
2271 [44]	2270 (m)	$\nu_1(A_1)$		2336 (22)	2229 (13) [215] <sup>[e]</sup>
2211 [8]	2210 (s)	$\nu_7(B_2)$		2282 (147)	2175 (105) [42]
	1088 (s)	$\nu_8(B_2)$		1167 (141)	1032 (138) [2]
871 [7]	872 (w)	$\nu_2(A_1)$		850 (4)	818 (0.5) [5]
	704 (vs)		$\nu_3(F_{1u})$		
686 [100]	680 (sh)		$\nu_1(A_{1g})$		
672 [17], 669 [18]		$\nu_3(A_1)$	or part of $\nu_1(A_{1g})$ or $\nu_3(F_{1u})$	678 (1)	644 (2) [1]
579 [16]	575 (w)		$\nu_2(E_g)$		
		$\nu_5(A_2)$		502 (0)	475 (0) [1]
	420 (sh)	$\nu_6(B_1)$		424 (7)	405 (6) [0]
		$\nu_9(B_2)$		436 (0.6)	399 (1) [0.5]
	394 (vs)		$\nu_4(F_{1u})$		
372 [32]	360 (sh), 380 (sh)		$\nu_5(F_{2g})$		
209 [44]		$\nu_4(A_1)$		193 (0.5)	181 (0.3) [6]
127 [55]		lattice vibration			

[a] Relative IR and Raman intensities given in parentheses and brackets, respectively. [b] Frequencies calculated using a 6–311 + G(2d) basis set. IR intensities given in parentheses [ $\text{km mol}^{-1}$ ], and Raman intensities given in brackets [ $\text{\AA}^4 \text{amu}^{-1}$ ]. [c]  $T = -130^\circ\text{C}$ . [d]  $T = -196^\circ\text{C}$ . [e] The Raman intensities were calculated at the RHF level.

Table 3. Comparison of the calculated (B3LYP) and observed  $^{15}\text{N}$  isotopic shifts for  $\text{N}_5^+$ .

$\text{N}_5^+$ isotopomer	$\nu_4(\text{A}_1)$	$\nu_9(\text{B}_2)$	$\nu_6(\text{B}_1)$	Calcd frequencies (shifts) [ $\text{cm}^{-1}$ ]					$\nu_8(\text{B}_2)$	$\nu_7(\text{B}_2)$	$\nu_1(\text{A}_1)$
				$\nu_5(\text{A}_2)$	$\nu_3(\text{A}_1)$	$\nu_2(\text{A}_1)$					
$^{14}\text{N}^{14}\text{N}^{14}\text{N}^{14}\text{N}^{14}\text{N}$	193.1(0)	424.1(0)	436.3(0)	502.4(0)	678.1(0)	850.0(0)		1116.9(0)	2281.7(0)	2336.3(0)	
$^{14}\text{N}^{14}\text{N}^{14}\text{N}^{15}\text{N}^{14}\text{N}$	191.8(1.3)	422.0(2.1)	436.0(.2)	502.4(0)	677.5(.7)	833.3(16.7)		1138.0(28.9)	2281.2(.5)	2336.3(.1)	
$^{15}\text{N}^{14}\text{N}^{14}\text{N}^{14}\text{N}^{14}\text{N}$	190.8(2.2)	422.3 (1.8)	434.7(1.5)	500.7(1.7)	674.4(3.7)	847.4(2.6)		1163.4(3.5)	2259.8(21.9)	2324.5(11.9)	

$\text{N}_5^+$ isotopomer	Obsd frequencies (shifts) [ $\text{cm}^{-1}$ ] <sup>[a]</sup>					
	$\nu_2(\text{A}_1)$ , IR	$\nu_2(\text{A}_1)$ , RA	$\nu_7(\text{B}_2)$ , IR	$\nu_7(\text{B}_2)$ , RA	$\nu_1(\text{A}_1)$ , IR	$\nu_1(\text{A}_1)$ , RA
$^{14}\text{N}^{14}\text{N}^{14}\text{N}^{14}\text{N}^{14}\text{N}$	872(0)	871(0)	2210(0)	2211(0)	2271(0)	2271(0)
$^{14}\text{N}^{14}\text{N}^{14}\text{N}^{15}\text{N}^{14}\text{N}$	858(14)	855(16)	2209.8	2211(1)	2270.8	2271(0)
$^{15}\text{N}^{14}\text{N}^{14}\text{N}^{14}\text{N}^{14}\text{N}$	870(2)	869(2)	2189.0(21)	2190(21)	2259.0(12)	2259(12)

[a] RA = Raman.

Table 4. Results from the normal coordinate analysis<sup>[a]</sup> of  $\text{N}_5^+$ .

Approx. mode in point group $\text{C}_{2v}$			Frequency [ $\text{cm}^{-1}$ ]		Symmetry force constants <sup>[b]</sup> CCSD(T) (B3LYP)				Potential energy distribution <sup>[a]</sup> [%]
			obsd	calcd	$\text{F}_{11}$	$\text{F}_{22}$	$\text{F}_{33}$	$\text{F}_{44}$	CCSD(T)
				CCSD(T) (B3LYP)					
$\text{A}_1$	$\nu_1$	in-phase terminal stretches	2270	2229 (2336)	$\text{F}_{11}$	19.573(21.314)			93(1) + 6(2)
	$\nu_2$	sym. central stretch	872	818 (850)	$\text{F}_{22}$	0.702(0.843)	5.546(6.952)		62(2) + 23(3) + 13(4) + 2(1)
	$\nu_3$	central bending		644 (678)	$\text{F}_{33}$	-0.085(-0.137)	1.377(1.535)	1.540(1.427)	39(3) + 33(2) + 23(4) + 5(1)
	$\nu_4$	in-phase terminal bends	209	181 (193)	$\text{F}_{44}$	0.167(0.171)	0.204(0.312)	0.120(0.108)	64(4) + 37(3) - (2)
$\text{A}_1$	$\nu_5$	torsion		475 (502)	$\text{F}_{55}$	0.0266(0.0281)			100(5)
$\text{B}_1$	$\nu_6$	torsion		405 (424)	$\text{F}_{66}$	0.0236(0.0246)			100(6)
					$\text{F}_{77}$		$\text{F}_{88}$	$\text{F}_{99}$	
$\text{B}_2$	$\nu_7$	out-of-phase term stretch	2210	2175 (2282)	$\text{F}_{77}$	19.491(21.272)			96(7) + 4(8)
	$\nu_8$	asym. central stretch	1088	1032 (1167)	$\text{F}_{88}$	1.197(1.359)	4.780(5.927)		95(8) + 4(7)
	$\nu_9$	out-of-phase terminal bends		399 (436)	$\text{F}_{99}$	0.200(0.195)	0.085(0.159)	0.358(0.423)	99(9) + 1(8)

[a] The following symmetry coordinates were used for  $[\text{N}_1\text{N}_2\text{N}_3\text{N}_2'\text{N}_1']^+$ :  $\text{S}_1 = \nu(1-2) + \nu(1'-2')$ ;  $\text{S}_2 = \nu(2-3) + \nu(2'-3)$ ;  $\text{S}_3 = \delta(2-3-2')$ ;  $\text{S}_4 = \delta(1-2-3) + \delta(1'-2'-3)$ ;  $\text{S}_5 = \tau(1-2-3-2') + \tau(2-3-2'-1')$ ;  $\text{S}_6 = \tau(1-2-3-2') - \tau(2-3-2'-1')$ ;  $\text{S}_7 = \nu(1-2) - \nu(1'-2')$ ;  $\text{S}_8 = \nu(2-3) - \nu(2'-3)$ ;  $\text{S}_9 = \delta(1-2-3) - \delta(1'-2'-3)$ . [b] The two most important internal force constants, estimated from the calculated symmetry force constants and the observed frequencies are  $f_{(1-2)} = 20.08 \text{ mdyne } \text{\AA}^{-1}$  and  $f_{(2-3)} = 6.59 \text{ mdyne } \text{\AA}^{-1}$ . Stretching constants in  $\text{mdyne } \text{\AA}^{-1}$ , deformation constants in  $\text{mdyne } \text{\AA}^{-1} \text{ rad}^{-2}$ , and stretch-bend interaction constants in  $\text{mdyne } \text{rad}^{-1}$ .

former value is significantly lower than the  $22.4 \text{ mdyne } \text{\AA}^{-1}$  found for the  $\text{N}\equiv\text{N}$  bond in  $\text{N}_2$ ,<sup>[15]</sup> whereas the latter value is between those found for typical  $\text{N}-\text{N}$  single ( $f_{\text{N}-\text{N}} = 3.6 \text{ mdyne } \text{\AA}^{-1}$ ) and double bonds ( $f_{\text{N}=\text{N}} = 10.2 \text{ mdyne } \text{\AA}^{-1}$ ).<sup>[15]</sup> The strengthening of the  $\text{N}-\text{N}$  central bonds at the expense of the terminal bonds, as suggested by the resonance structures, explains the relative stability of  $\text{N}_5^+$  toward  $\text{N}_2$  elimination. Reliable calculations of the energy barrier for  $\text{N}_2$  elimination from  $\text{N}_5^+$  will be the subject of a separate study.

## Experimental Section

**Caution!**  $\text{N}_5^+\text{AsF}_6^-$  is a highly energetic, strongly oxidizing material that can detonate violently. It should be handled only on a very small scale while using appropriate safety precautions (face shields, leather gloves, and protective clothing).

The  $\text{N}_2\text{F}^+\text{AsF}_6^-$  was prepared from *cis*- $\text{N}_2\text{F}_2$  and  $\text{AsF}_5$  as previously described.<sup>[16a-c]</sup> The  $\text{HN}_3$  was generated by heating  $\text{NaN}_3$  with a threefold excess of stearic acid to about  $80^\circ\text{C}$  under a dynamic vacuum and collecting the evolved  $\text{HN}_3$  in a trap cooled with liquid  $\text{N}_2$ . The  $\text{HN}_3$  was purified by fractional condensation through a series of traps at  $-64$ ,  $-95$ , and  $-196^\circ\text{C}$ , with the material retained at  $-95^\circ\text{C}$  being used. Singly  $^{15}\text{N}$ -labeled  $\text{NaN}_3$  (Cambridge Isotope Laboratories, 99%  $^{15}\text{N}$  label) was used for the preparation of a roughly 50:50 mixture of  $\text{HN}_3$  that was singly  $^{15}\text{N}$ -labeled in either the  $\alpha$  or  $\gamma$  position. The HF (Matheson Co.) was dried by storage over  $\text{BiF}_3$ .<sup>[17]</sup>

The  $\text{HN}_3$  was generated and handled on a Pyrex glass vacuum line equipped with grease-free Kontes glass-Teflon valves. The HF was handled on a previously described<sup>[18]</sup> stainless steel-Teflon FEP vacuum line. The  $\text{N}_5^+\text{AsF}_6^-$  samples were handled at  $-196^\circ\text{C}$  in the dry  $\text{N}_2$  atmosphere of a glove box.

Low-temperature Raman spectra were recorded on a Cary Model 83GT spectrometer using the 488-nm line of an Ar-ion laser for excitation, a previously described cooling device,<sup>[19]</sup> and quartz tubes (3 mm outer diameter) as sample containers. For measurements of the  $^{14}\text{N}-^{15}\text{N}$  isotopic shifts, the signal was scale expanded on an external strip chart recorder. The low-temperature IR spectra were recorded on a Mattson Galaxy FTIR

spectrometer using a demountable low-temperature cell equipped with CsI windows. The  $^{14}\text{N}$  and  $^{15}\text{N}$  NMR spectra were recorded at 36.13 and 50.69 MHz, respectively, on a Bruker AMX 500 spectrometer using saturated solutions of  $\text{N}_5^+\text{AsF}_6^-$  in  $\text{HF}/\text{AsF}_5$  at  $-63^\circ\text{C}$  and heat-sealed 5-mm Teflon-FEP liners (Wilma Glass Co.) as sample containers, delay times of 60–120 s for the recording of the  $^{15}\text{N}$  spectra, and neat  $\text{CH}_3\text{NO}_2$  and aqueous  $^{15}\text{N}$ -labeled urea referenced as  $\delta = -305.0$  relative to  $\text{CH}_3\text{NO}_2$  as external standards. The spectra were recorded both  $^1\text{H}$ -coupled and  $^1\text{H}$ -decoupled to determine if there was a nuclear Overhauser effect.

**Preparation of  $\text{N}_5^+\text{AsF}_6^-$ :** In a typical experiment,  $\text{N}_2\text{F}^+\text{AsF}_6^-$  (1.97 mmol) was loaded in the drybox into a Teflon-FEP ampule (1.9 cm outer diameter) that was closed by a stainless steel valve. On the metal vacuum line, anhydrous HF ( $\approx 3$  mL) was added at  $-196^\circ\text{C}$ , and the mixture was warmed to room temperature to dissolve the  $\text{N}_2\text{F}^+\text{AsF}_6^-$ . The ampule was connected to the glass line, and  $\text{HN}_3$  (2.39 mmol) was added at  $-196^\circ\text{C}$ . The ampule was reconnected to the metal line and allowed to warm to  $-78^\circ\text{C}$ , where it was kept for three days with occasional gentle agitation. The ampule was then cooled to  $-196^\circ\text{C}$  to check for the presence of volatile products. Nitrogen (0.76 mmol) was identified by mass spectrometry. All material volatile at  $-64^\circ\text{C}$  was pumped off for 8 h, leaving behind a white solid residue that was identified by low-temperature vibrational and  $^{14}\text{N}$  and  $^{15}\text{N}$  NMR spectroscopy as a mixture of  $\text{N}_5^+\text{AsF}_6^-$  ( $\approx 80$  mol %) and  $\text{H}_2\text{N}_3^+\text{AsF}_6^-$  ( $\approx 20$  mol %).

**Preparation of  $^{15}\text{N}$ -labeled  $\text{N}_5^+\text{AsF}_6^-$ :** The procedure was identical to that used for the synthesis of unlabeled  $\text{N}_5^+\text{AsF}_6^-$ , except for the use of a mixture of  $\text{HN}_3$  that was  $^{15}\text{N}$ -labeled in either the  $\text{N}_\alpha$  or  $\text{N}_\gamma$  position.

**Computational Methods.** Hartree–Fock (HF), density functional theory (DFT), and single- and double-excitation coupled cluster calculations<sup>[20]</sup> that include a noniterative treatment of connected triple excitations (denoted CCSD(T))<sup>[21]</sup> were carried out employing several atomic basis sets. The DFT calculations employed the B3LYP functional.<sup>[22]</sup> Geometries, IR and Raman spectra, and nuclear magnetic resonance shieldings were calculated for  $\text{N}_5^+$  as well as (for calibration purposes)  $\text{N}_2\text{F}^+$ ,  $\text{H}_2\text{N}_3^+$ , and the standard  $\text{CH}_3\text{NO}_2$ , the geometries and NMR parameters of which are experimentally known.<sup>[12, 14, 16]</sup> The vibrational spectra reported in this work were computed using the 6-311 + G(2d) atomic basis set.<sup>[23]</sup> The NMR shieldings were computed at the CCSD(T)/6-311 + G(2d) geometries employing the gauge-including atomic orbital (GIAO) solution to the gauge-invariance problem<sup>[24]</sup> and density matrices obtained from second-order many-body perturbation theory [MBPT(2)], CCSD, or CCSD(T) calculations.<sup>[25–27]</sup> The results reported in this work used quadruple-zeta plus polarization (QZP) atomic basis sets derived from the QZ sets of Schäfer et al.,<sup>[28]</sup> supplemented with a d function with exponent 1.0. As discussed by Gauss and Stanton,<sup>[25–27]</sup> the accurate calculation of nitrogen NMR shieldings frequently requires an extensive electron correlation treatment such as that provided by the CCSD(T) method. Hartree–Fock and even MBPT(2) shielding calculations for species such as  $\text{N}_5^+$  with many free valence electron pairs yield extremely poor results. The GAMESS,<sup>[29]</sup> Gaussian,<sup>[30]</sup> and ACES II<sup>[31]</sup> program systems were used for these calculations on IBM RS/6000 work stations.

Received: March 9, 1999 [Z13131IE]

German version: *Angew. Chem.* **1999**, *111*, 2112–2118

**Keywords:** density functional calculations • isotopic labeling • nitrogen • NMR spectroscopy • vibrational spectroscopy

- [1] See, for example, *Proceedings of the High Energy Density Matter Conference* (New Orleans, LA) **1989**, available from the Defense Technical Information Center, Fort Belvoir, VA, as report no. ADA212314.
- [2] W. J. Lauderdale, J. F. Stanton, R. J. Bartlett, *J. Phys. Chem.* **1992**, *96*, 1173.
- [3] M. N. Glukhovtsev, H. Jiao, P. v. R. Schleyer, *Inorg. Chem.* **1996**, *35*, 7124.
- [4] For a recent summary of previous experimental and theoretical studies, see the citations given in reference [3], and M. T. Nguyen, T. K. Ha, *Chem. Ber.* **1996**, *129*, 1157.

- [5] a) T. Curtius, *Ber. Dtsch. Chem. Ges.* **1890**, *23*, 3023; b) N. N. Greenwood, A. Earnshaw, *Chemistry of the Elements*, Pergamon, Oxford, **1984**, p. 466.
- [6] For a recent summary of previous work, see J. Wasilewski, *J. Chem. Phys.* **1996**, *105*, 10969.
- [7] a) R. Tian, J. C. Facelli, J. Michl, *J. Phys. Chem.* **1988**, *92*, 4073; b) J. A. Guthrie, R. C. Chaney, A. J. Cunningham, *J. Chem. Phys.* **1991**, *95*, 930.
- [8] a) W. E. Thompson, M. E. Jacox, *J. Chem. Phys.* **1990**, *93*, 3856; b) E. Bieske, *J. Chem. Phys.* **1993**, *98*, 8537; c) K. Sohlberg, *J. Mol. Struct. (Theochem.)* **1995**, *339*, 195; d) T. Ruchti, T. Speck, J. P. Connelly, E. J. Bieske, H. Linnartz, J. P. Maier, *J. Chem. Phys.* **1996**, *105*, 2591.
- [9] F. A. Cotton, G. Wilkinson, *Advanced Inorganic Chemistry*, 3rd ed., Interscience, New York, **1972**, p. 113.
- [10] P. Pyykkö, N. Runeberg, *J. Mol. Struct. (Theochem.)* **1991**, *234*, 279.
- [11] G. Rasul, private communication.
- [12] K. O. Christe, W. W. Wilson, D. A. Dixon, S. I. Khan, R. Bau, T. Metzenthin, R. Lu, *J. Am. Chem. Soc.* **1993**, *115*, 1836.
- [13] L. A. Curtiss, K. Raghavachari, G. W. Trucks, J. A. Pople, *J. Chem. Phys.* **1991**, *94*, 7221.
- [14] K. O. Christe, J. F. Hon, D. Pilipovich, *Inorg. Chem.* **1973**, *12*, 84.
- [15] a) H. Siebert, *Anwendungen der Schwingungsspektroskopie in der Anorganischen Chemie, Anorganische und Allgemeine Chemie in Einzeldarstellungen VII*, Springer, Heidelberg, **1996**; b) J. Weidlein, U. Müller, K. Dehnicke, *Schwingungsspektroskopie*, Georg Thieme, Stuttgart, **1982**.
- [16] a) D. Moy, A. R. Young, *J. Am. Chem. Soc.* **1965**, *87*, 1889; b) K. O. Christe, R. D. Wilson, W. Sawodny, *J. Mol. Struct.* **1971**, *8*, 245; c) K. O. Christe, R. D. Wilson, W. W. Wilson, R. Bau, S. Sukumar, D. A. Dixon, *J. Am. Chem. Soc.* **1991**, *113*, 3795; d) J. Mason, K. O. Christe, *Inorg. Chem.* **1983**, *22*, 1849.
- [17] K. O. Christe, W. W. Wilson, C. J. Schack, *J. Fluorine Chem.* **1978**, *11*, 71.
- [18] K. O. Christe, R. D. Wilson, C. J. Schack, *Inorg. Synth.* **1986**, *24*, 3.
- [19] F. A. Miller, B. M. Harney, *Appl. Spectrosc.* **1970**, *24*, 291.
- [20] G. D. Purvis III, R. J. Bartlett, *J. Chem. Phys.* **1982**, *76*, 1910.
- [21] K. Raghavachari, G. W. Trucks, J. A. Pople, M. Head-Gordon, *Chem. Phys. Lett.* **1989**, *157*, 479.
- [22] A. D. Becke, *J. Chem. Phys.* **1993**, *98*, 5648.
- [23] M. J. Frisch, J. A. Pople, J. S. Binkley, *J. Chem. Phys.* **1984**, *80*, 3265.
- [24] R. Ditchfield, *Mol. Phys.* **1974**, *27*, 789.
- [25] J. Gauss, *J. Chem. Phys.* **1993**, *99*, 3629.
- [26] J. Gauss, J. F. Stanton, *J. Chem. Phys.* **1995**, *103*, 3561.
- [27] J. Gauss, J. F. Stanton, *J. Chem. Phys.* **1996**, *104*, 2574.
- [28] A. Schäfer, H. Horn, R. Ahlrichs, *J. Chem. Phys.* **1992**, *97*, 2571.
- [29] GAMESS, M. W. Schmidt, K. K. Baldrige, J. A. Boatz, S. T. Elbert, M. S. Gordon, J. J. Jensen, S. Koseki, N. Matsunaga, K. A. Nguyen, S. Su, T. L. Windus, M. Dupuis, J. A. Montgomery, *J. Comput. Chem.* **1993**, *14*, 1347.
- [30] Gaussian 94, Revision E.2, M. J. Frisch, G. W. Trucks, H. B. Schlegel, P. M. W. Gill, B. G. Johnson, M. A. Robb, J. R. Cheeseman, J. Keith, G. A. Petersson, J. A. Montgomery, K. Raghavachari, M. A. Al-Laham, V. G. Zakrzewski, J. V. Ortiz, J. B. Foresman, J. Cioslowski, B. B. Stefanov, A. Nanayakkara, M. Challacombe, C. Y. Peng, P. Y. Ayala, W. Chen, M. W. Wong, J. L. Andres, E. S. Replogle, R. Gomperts, R. L. Martin, D. J. Fox, J. S. Binkley, D. J. Defress, J. Baker, J. P. Stewart, M. Head-Gordon, C. Gonzalez, J. A. Pople, Gaussian, Inc., Pittsburgh, PA, **1995**.
- [31] ACES II, Quantum Theory Project, University of Florida. Authors: J. F. Stanton, J. Gauss, J. D. Watts, M. Noijen, N. Oliphant, S. A. Perera, P. G. Szalay, W. J. Lauderdale, S. R. Gwaltney, S. Beck, A. Balkova, D. E. Bernholdt, K. K. Baeck, P. Rozyczko, H. Sekino, C. Hober, R. J. Bartlett; integral packages included are VMOL (J. Almlöf, P. R. Taylor), BPROPS (P. R. Taylor), and ABACUS (T. Helgaker, H. J. Aa. Jensen, P. Jorgensen, J. Olsen, P. R. Taylor).